Received 19 October 2020
Revised 20 January 2021
4 February 2021
Accepted 7 February 2021

Fast and reliable knowledge-based design closure of antennas by means of iterative prediction-correction scheme

Slawomir Koziel
Department of Engineering Optimization and Modeling, Center of Reykjavik University, Reykjavik, Iceland, and

Anna Pietrenko-Dabrowska
Faculty of Electronics, Telecommunications and Informatics, Gdansk University of Technology, Gdansk, Poland

Abstract

Purpose – A novel framework for expedited antenna optimization with an iterative prediction-correction scheme is proposed. The methodology is comprehensively validated using three real-world antenna structures: narrow-band, dual-band and wideband, optimized under various design scenarios.

Design/methodology/approach – The keystone of the proposed approach is to reuse designs pre-optimized for various sets of performance specifications and to encode them into metamodels that render good initial designs, as well as an initial estimate of the antenna response sensitivities. Subsequent design refinement is realized using an iterative prediction-correction loop accommodating the discrepancies between the actual and target design specifications.

Findings – The presented framework is capable of yielding optimized antenna designs at the cost of just a few full-wave electromagnetic simulations. The practical importance of the iterative correction procedure has been corroborated by benchmarking against gradient-only refinement. It has been found that the incorporation of problem-specific knowledge into the optimization framework greatly facilitates parameter adjustment and improves its reliability.

Research limitations/implications – The proposed approach can be a viable tool for antenna optimization whenever a certain number of previously obtained designs are available or the designer finds the initial effort of their gathering justifiable by intended re-use of the procedure. The future work will incorporate response features technology for improving the accuracy of the initial approximation of antenna response sensitivities.

Originality/value – The proposed optimization framework has been proved to be a viable tool for cost-efficient and reliable antenna optimization. To the knowledge, this approach to antenna optimization goes beyond the capabilities of available methods, especially in terms of efficient utilization of the existing

This work was supported in part by the Icelandic Center for Research (RANNIS) Grant 206606051 and by the National Science Center of Poland Grant 2017/27/B/ST7/00563. The authors would like to thank Dassault Systemes, France, for making CST Microwave Studio available.

Engineering Computations
Vol. 38 No. 10, 2021
pp. 3710-3731
Emerald Publishing Limited
0264-4401
DOI 10.1108/EC-10-2020-0600

knowledge, thus enabling reliable parameter tuning over broad ranges of both operating conditions and material parameters of the structure of interest.

Keywords Kriging interpolation, EM simulation, Design closure, Iterative correction, Knowledge-based optimization, Parameter tuning, Antenna design

Paper type Research paper

1. Introduction

Steadily increasing performance requirements have made the design of contemporary antenna structures a challenging endeavor. These growing demands do not only pertain to electrical or field characteristics (Aldhafeeri and Rahmat-Samii, 2019; Liao *et al.*, 2015) but also the implementation of additional functionalities such as multi-band operation (Deshmukh *et al.*, 2019), pattern/polarization diversity (Saurav *et al.*, 2018), band notches (Xu *et al.*, 2018), circular polarization (Kumar *et al.*, 2019), tunability (Huang *et al.*, 2015), or – more often than not – size reduction (Kim and Nam, 2019; Li *et al.*, 2018). The important stimulus here is the emergence of new application areas including the internet of things (IoT) (Salam *et al.*, 2019), mobile communications (especially 5 G; Zeng and Luk, 2019), medical imaging (Connell and Menon, 2019; Felicio *et al.*, 2019) or wearable/implantable devices (Mendes and Peixeiro, 2018). The need for meeting stringent specifications fosters the development of antennas of increasingly complex geometries. This strongly affects the design practices, in particular, emphasizes the role of full-wave electromagnetic (EM) simulation tools (Wu and Sarabandi, 2017; Han *et al.*, 2017). In many cases, beyond the early conceptual development, the design process is entirely EM-driven, that including topology evolution (Ullah and Koziel, 2018), initial adjustments through parameter sweeping (Bhattacharya *et al.*, 2016) and design closure (Fakih *et al.*, 2019). The latter is more and more frequently realized by means of rigorous numerical optimization. This is virtually imperative when multiple variables, performance figures and constraints need to be handled simultaneously (Dong *et al.*, 2019). Notwithstanding, multiple antenna evaluations required by the optimization algorithms incur considerable computational overhead. This may become a serious bottleneck even for a local search, let alone global optimization (in particular, population-based algorithms such as particle swarm optimization (Lalbakhsh *et al.*, 2017), differential evolution (Goudos *et al.*, 2011) or genetic algorithms (Choi *et al.*, 2016), as well as uncertainty quantification or statistical design (Du and Roblin, 2018; Kouassi *et al.*, 2016).

Under these circumstances, expediting simulation-based design procedures has been a focus of extensive research over the recent years (Hassan *et al.*, 2015 through Torun and Swaminathan, 2019). Some of the promising directions include algorithmic developments (e.g. incorporation of adjoint sensitivities into gradient search algorithms (Hassan *et al.*, 2015; Wang *et al.*, 2018), sparse sensitivity updates (Koziel and Pietrenko-Dabrowska, 2019a, 2019b), application of fast analysis techniques (typically targeting particular classes of the antenna structures, e.g. Tsukamoto and Arai (2016), Arndt (2012) or machine learning methods (Alzahed *et al.*, 2019; Tak *et al.*, 2018), as well as exploitation of a particular structure of antenna responses (feature-based optimization (Koziel, 2015)). Surrogate-assisted frameworks constitute another branch of quickly growing popularity (Baratta *et al.*, 2018 through Torun and Swaminathan, 2019). These methods may involve both physics-based models (space mapping (Baratta *et al.*, 2018), adaptive response scaling (Koziel and Unnsteinsson, 2018) and data-driven (approximation) surrogates (kriging interpolation, Easum *et al.* (2018); support vector regression, Jacobs (2012); Gaussian process regression, Jacobs and Koziel (2014) or artificial neural networks, Mishra *et al.* (2015), also in combination with sequential sampling methods (Torun and Swaminathan, 2019).

One of the scenarios of practical importance is re-design (or dimension scaling) of a particular structure for different operating conditions (e.g. operating frequencies in the case of multi-band antennas) or material parameters (e.g. substrate height or dielectric permittivity in the case of planar structures). When executed without prior problem-specific knowledge, the re-design process faces the same challenges and entails similar CPU costs as those associated with finding the original design (or designs). Using previously obtained designs may expedite the optimization process. One possibility is analytical design curves that determine the relationships between the performance figures and geometry parameters and permit rapid identification of at least a decent initial design (Caenepeel *et al.*, 2016). Recently, the utilization of inverse surrogate models has been fostered for that purpose (Leifsson and Koziel, 2014), also using variable-fidelity EM simulation models (Ullah *et al.*, 2020).

This paper presents a novel knowledge-based methodology for low-cost and reliable optimization of antenna structures. Our procedure incorporates the problem-specific information (in the form of pre-existing designs, e.g. optimized for various sets of performance specifications) into the machine learning framework involving data-driven (here, kriging interpolation) metamodels. These surrogates are used to render the initial point but also to produce an approximation of the sensitivity matrix, which accelerates subsequent design refinement. To further reduce the computational overhead of the optimization process and improve its reliability, an iterative correction procedure is developed that feeds the discrepancies between the actual and the target performance figure values back to the surrogate. The latter returns an improved parameter vector at a cost of a single EM antenna analysis per iteration. The proposed methodology is demonstrated using three-antenna structures: a dual-band dipole, a quasi-Yagi antenna with a parabolic reflector and a wideband monopole, all optimized under various design scenarios. The obtained numerical results corroborate the efficacy of our approach, the importance of using the available problem-specific knowledge, as well as illustrates the advantages of the presented procedure over gradient-based design refinement. The average cost of producing an optimized design is only a few evaluations of the EM antenna model.

The originality and technical contributions of this work include the development of an automated and reliable machine learning optimization framework using pre-existing knowledge on the antenna structure at hand, development of iterative correction procedure for rapid design refinement, demonstration of a possibility of expedited design while handling various performance figures and operating conditions (e.g. operating frequencies, realized gain, substrate permittivity), demonstrated capability of quasi-global design closure using primarily local methods.

2. Fast design closure using machine learning and iterative correction

This section formulates the proposed knowledge-based design closure methodology. One of its distinctive features is the incorporation of available information about the antenna of interest in the form of previously obtained designs, either available from the previous work with the structure or prepared specifically to set up the framework. This information is blended into a kriging surrogate model which yields – for a given target vector of performance figures – a reasonably good initial design (Section 2.2). The second feature is an iterative correction procedure for rapid design refinement. The latter is achieved by feeding the surrogate with the accumulated discrepancies between the target performance figure values and those extracted from the design produced in the previous iteration.

2.1 Design closure task. Objective space

Let $\boldsymbol{x} \in X$ denote a vector of adjustable parameters, where X is the parameter space of the antenna of interest. A certain number of performance figures, F_k, $k = 1, \ldots, N$, is considered.

The typical figures may be target operating frequencies, minimum acceptable fractional bandwidth, minimization of the sidelobe level, maximization of gain but also other conditions, e.g. parameters of the dielectric substrate (thickness, permittivity). The intended ranges $F_{k.\min} \leq F_k \leq F_{k.\max}$ for F_k determine the objective space F, i.e. the region in which the design closure framework is supposed to operate.

We denote by $\boldsymbol{R}(x)$ the output of the EM simulation antenna model, typically a set of vectors containing the relevant characteristics such as reflection, gain, etc. A scalar merit function $U(\boldsymbol{R}(x))$ measures the quality of the design $\boldsymbol{x}$ with respect to the objective vector $\boldsymbol{F} = [F_1 \ldots F_N]^T$. An example follows. Suppose that the goal is to allocate the resonances of a dual-band antenna at the target frequencies $f_{0.1}$ and $f_{0.2}$ in the sense of maintaining $|S_{11}(\boldsymbol{x}, \boldsymbol{f})| \leq -10$ dB within the fractional bandwidths B (symmetric w.r.t. $f_{0.k}$, $k = 1,2$) and to maximize the average realized gain $G(\boldsymbol{x}, f)$ within the same bandwidths. In this case, the figures of interests are $F_k = f_{0.k}$, $k = 1, 2$, whereas the function U may be defined as:

$$U(\boldsymbol{R}(\boldsymbol{x}), \boldsymbol{F}) = -\sum_{k=1}^{2} (Bf_{0.k})^{-1} \int_{f_{0.k}(1-B/2)}^{f_{0.k}(1+B/2)} G(\boldsymbol{x}, f)df + \\ + \sum_{k=1}^{2} \beta_k \left[\max \left\{ \frac{\max\{f \in B_k : |S_{11}(\boldsymbol{x}, f)|\} + 10}{10}, 0 \right\} \right]^2 \tag{1}$$

where $B_k = [f_{0.k}(1 - B/2), f_{0.k}(1 + B/2)]$ and β_k are the penalty factors. Here, the first component is the average in-band gain, whereas the second component constitutes penalty functions activated if the condition $|S_{11}(\boldsymbol{x}, \boldsymbol{f})| \leq -10$dB is violated in any of the operating bands.

Having defined the objective space and the merit function, the design optimality can be formulated as a solution to the following nonlinear minimization problem:

$$\boldsymbol{x}^* = \arg\min_{\boldsymbol{x}} U(\boldsymbol{R}(\boldsymbol{x}), \boldsymbol{F}) \tag{2}$$

2.2 Incorporating problem-specific knowledge

The assumption is that a certain number of designs are already available from the previous work with the same antenna structure. These designs are denoted as $\boldsymbol{x}_b^{(j)}$, $j = 1, \ldots, p$ and optimized for the objective vectors $\boldsymbol{F}^{(j)} = \left[F_1^{(j)} \ldots F_N^{(j)}\right]^T$ according to (2). The symbol $\boldsymbol{J}_b^{(j)} = \boldsymbol{J}\left(\boldsymbol{x}_b^{(j)}\right)$, $j = 1, \ldots, p$, will stand for the Jacobian matrices of the antenna characteristics at the designs $\boldsymbol{x}_b^{(j)}$. This data is normally available as a by-product of solving (2). From the point of view of balanced coverage of the objective space, if possible, the vectors $F^{(j)}$ should be allocated uniformly within the objective space F.

2.3 Initial design rendition by machine learning

Given the pre-existing data as described in Section 2.2, the following kriging interpolation (Queipo *et al.*, 2005) models are constructed:

- $\boldsymbol{s}_x(\cdot)$, mapping the objective space F into the parameter space X; identification of the surrogate $\boldsymbol{s}_x(\cdot)$ is based on the data pairs $\{\boldsymbol{F}^{(j)}, \boldsymbol{x}_b^{(j)}\}_{j=1,\ldots,p}$;
- $\boldsymbol{s}_J(\cdot)$, mapping the objective space F into the space of the system response sensitivities; this model is rendered using $\{\boldsymbol{F}^{(j)}, J_b^{(j)}\}_{j=1,\ldots,p}$ as the training set.

The purpose of the model $\boldsymbol{s}_x$ is to approximate the region of the parameter space X containing the designs optimal with respect to F in the sense of (2). Because a limited amount of data is used to identify the surrogate (i.e. p optimum points $\boldsymbol{x}_b^{(j)}$), the design $\boldsymbol{s}_x(\boldsymbol{F})$ does not generally coincide with $\arg\min\{\boldsymbol{x}: \boldsymbol{U}(\boldsymbol{R}(x), \boldsymbol{F})\}$, i.e. the design optimum w.r.t. the objective vector $\boldsymbol{F}$. Notwithstanding, this is the best information we have at this stage of the process. Consequently, the initial design corresponding to a given target objective vector $\boldsymbol{F}_t$ will be assigned as:

$$\boldsymbol{x}^{(0)} = \boldsymbol{s}_x(\boldsymbol{F}_t) \tag{3}$$

Similarly, the approximate sensitivity matrix of the antenna characteristics at the design $\boldsymbol{x}^{(0)}$ is obtained as:

$$\boldsymbol{J}^{(0)} = \boldsymbol{s}_J(\boldsymbol{F}_t) \tag{4}$$

Figure 1 provides a graphical illustration of the considered concepts for $N = 2$ (two-dimensional objective space F) and $n = 3$ (three-dimensional parameter space X).

2.4 Gradient-based design refinement

As mentioned above, the initial design (3) has to be improved because $\boldsymbol{s}_x(F) \neq O(F)$ (the set of optimum designs w.r.t. all $\boldsymbol{F} \in F$). Here, the basic refinement procedure involves local

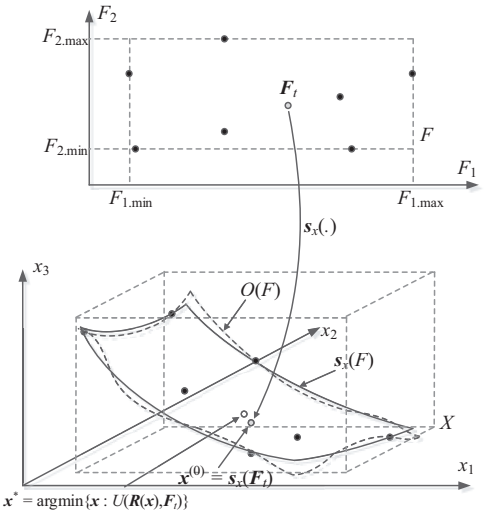

Figure 1.
Basic concepts of the presented design closure framework: (top picture) the objective space F and the exemplary target objective vector $\boldsymbol{F}_t$; (bottom picture): $\boldsymbol{s}_x(F)$ (solid lines), the set of optimum designs $O(F)$ (dashed lines) and the exemplary initial design $\boldsymbol{s}_x(\boldsymbol{F}_t)$ (gray-shaded circle) corresponding to the target objective or $\boldsymbol{F}_t$. Designs and $\boldsymbol{s}_x(\boldsymbol{x}_b^{(j)})$ are ked using black es. As $\boldsymbol{s}_x(F)$ is an roximation of : $\arg\min\{\boldsymbol{x}: U(\boldsymbol{R}$ $_t)\}$, $\boldsymbol{x}^*$ (white e) does not cide with $\boldsymbol{s}_x(\boldsymbol{F}_t)$

optimization realized using the trust-region gradient-based algorithm (Conn *et al.*, 2000). The algorithm produces a series of approximations $\boldsymbol{x}^{(i)}$, $i = 0,1,\ldots$ to x^* as:

$$\boldsymbol{x}^{(i+1)} = \arg \min_{\boldsymbol{x};\, -\boldsymbol{d}^{(i)} \le \boldsymbol{x}-\boldsymbol{x}^{(i)} \le \boldsymbol{d}^{(i)}} U\left(\boldsymbol{L}^{(i)}(\boldsymbol{x}), \boldsymbol{F}_t\right) \tag{5}$$

where $\boldsymbol{L}^{(i)}(\boldsymbol{x}) = \boldsymbol{R}(\boldsymbol{x}^{(i)} + \boldsymbol{J}(\boldsymbol{x}^{(i)}) \cdot (\boldsymbol{x} - \boldsymbol{x}^{(i)})$ is the first-order Taylor expansion of $\boldsymbol{R}(\boldsymbol{x})$ obtained using the Jacobian $\boldsymbol{J}$ at $\boldsymbol{x}^{(i)}$.

The computational cost of (5) is at least $n + 1$ EM antenna simulations per iteration assuming that the Jacobian is obtained using finite differentiation. Here, this cost is reduced to one EM analysis per iteration by jump-starting the process using the sensitivity matrix estimation with (4) and updating the Jacobian using the Broyden formula (Broyden, 1965) in subsequent iterations.

A practical issue of the refinement through (5) is that it might be prone to a failure if the initial design produced by (3) is away from $O(F)$, i.e. the true optimum or the quality of Jacobian estimation (4) is poor. Also, (5) may not be capable of correcting large frequency shifts (e.g. inaccurate allocation of operating frequencies obtained by (3)).

2.5 Iterative correction procedure

Given the deficiencies of the gradient-based refinement procedure as outlined in Section 2.4, an alternate scheme is proposed. It is a derivative-free correction process that involves multiple evaluations of the surrogate model $\boldsymbol{s}_x$.

We denote by $\boldsymbol{F}_{tmp.0}$ the objective vector that has been extracted from the EM-simulated antenna response at the design $\boldsymbol{x}^{(0)}$ of (3). For example, if the figures of interest are the target center frequencies of a multi-band antenna, $\boldsymbol{F}_{tmp.0}$would consists of the actual center frequencies of $\boldsymbol{R}(\boldsymbol{x}^{(0)})$. The design "inaccuracy" in terms of the assumed figures of interest can be then quantified as $\Delta\boldsymbol{F}^{(0)} = \boldsymbol{F}_{tmp.0} - \boldsymbol{F}_t$. The surrogate $\boldsymbol{s}_x$ can be reused to produce the corrected design:

$$\boldsymbol{x}^{(1)} = s_x\left(\boldsymbol{F}_t - \Delta\boldsymbol{F}^{(0)}\right) \tag{6}$$

which brings us closer to the optimum design manifold $O(F)$. Clearly, the dependence between the antenna parameters and its figures of interest is not linear; therefore, the process (6) has to be iterated by taking into account the accumulated errors. The sequence of corrected designs is generated accordingly as:

$$\boldsymbol{x}^{(i+1)} = s_x\left(\boldsymbol{F}_t - \sum_{k=0}^{i} \Delta\boldsymbol{F}^{(k)}\right) \tag{7}$$

where $\Delta\boldsymbol{F}^{(k)} = \boldsymbol{F}_{tmp.k} - \boldsymbol{F}_t$ and $\boldsymbol{F}_{tmp.k}$ denotes the vector containing the objectives extracted from the EM-simulated antenna response for the design $\boldsymbol{x}^{(k)}$. Figure 2 shows the graphical illustration of the first two iterations of (7).

Because (7) is capable of making relatively large design relocations, therefore, typically, the process converges after a few iterations. Furthermore, (7) permits correcting considerable frequency shifts, which is difficult (or slow at the least) by means of (5), mostly due to using approximate Jacobians. For this very reason, (7) will likely be computationally cheaper than the gradient-based optimization. On the other hand, re-evaluation of the surrogate $\boldsymbol{s}_x$ primarily affects those figures of interest that define the objective space F (e.g.

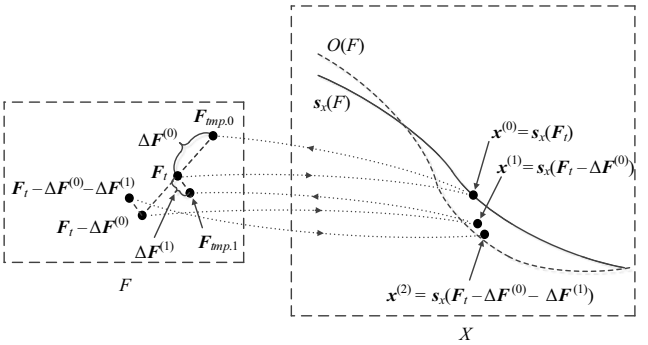

Figure 2.
Conceptual illustration of the iterative correction procedure (here, shown for $N = 2$ and $n = 1$)

Notes: The initial design lies on $\boldsymbol{s}_x(F)$ and its corresponding performance figure vector $F_{tmp.0}$ does not coincide with the target vector $\boldsymbol{F}_t$ because $\boldsymbol{s}_x(F) \neq O(F)$. The next design $\boldsymbol{x}^{(1)}$ is closer to $O(F)$ due to accommodating the discrepancy $\Delta F(0)$ into $\boldsymbol{s}_x$. Further improvement is obtained in the second iteration of the procedure

the location of the resonances of multi-band antennas but not the resonance depths). Consequently, further parameter tuning that operates at the level of antenna characteristics (i.e. as in (2)), might be required. Here, it is realized using the trust-region algorithm (5) as a follow-up procedure.

The flowchart of the entire optimization framework has been shown in Figure 3. It should be emphasized that because the domain of the models $\boldsymbol{s}_x$ and $\boldsymbol{s}_f$ is the entire objective space F, the framework exhibits global search properties within the relevant ranges of performance figures.

3. Verification examples

This section provides numerical and experimental verification of the presented knowledge-based design closure framework. It is based on three antenna structures: a uniplanar dual-band dipole, a quasi-Yagi antenna and a wideband monopole antenna. In each case, a different design scenario is considered as discussed in Sections 3.1 through 3.3. The simulation models of all the antennas from the benchmark set have been implemented in CST Microwave Studio. Notwithstanding, the actual choice of the simulation package is of secondary importance and virtually any available commercial solver such as HFSS or ADS may be used as a simulation tool within the proposed framework.

3.1 Case 1: Uniplanar dipole antenna

The first example is a dual-band uniplanar dipole antenna (Antenna I), shown in Figure 4 Chen *et al.* (2006), implemented on RO4350 substrate (ε_r = 3.5, h = 0.76 mm) and fed by a 50 Ohm coplanar waveguide (CPW). The adjustable parameters are $\boldsymbol{x} = [l_1\ l_2\ l_3\ w_1\ w_2\ w_3]^T$. Other parameters are fixed: l_0 = 30, w_0 = 3, s_0 = 0.15 and o = 5 (all dimensions in mm). The EM model $\boldsymbol{R}$ (~100.000 cells; simulation time 60 s) is implemented in CST Microwave Studio and evaluated using its time-domain solver.

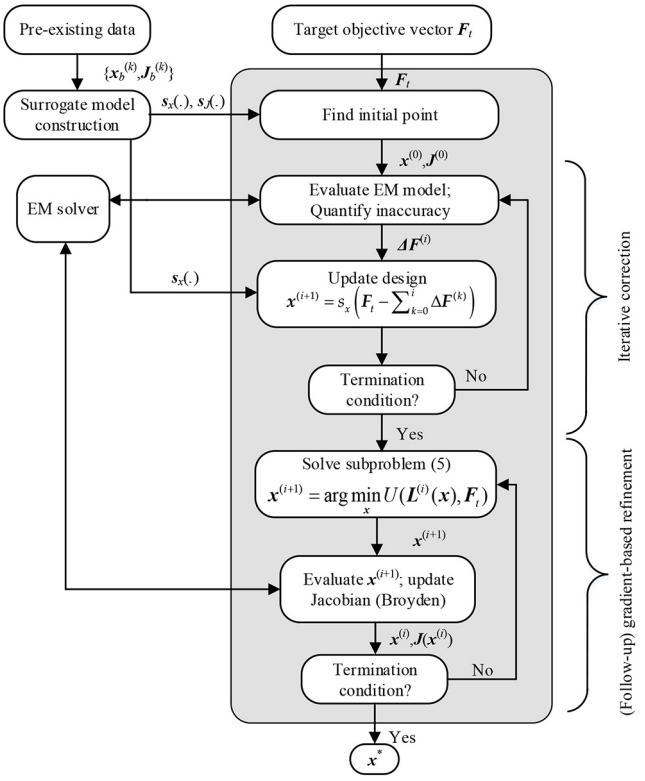

Figure 3.
Flow diagram of the proposed knowledge-based design closure framework

The design problem is to allocate the antenna resonances at the required operating frequencies f_1 and f_2 and, simultaneously, to improve the impedance matching at and around both f_1 and f_2. The ranges of interest are 2.0 GHz $\leq f_1 \leq$ 3.0 GHz (lower band) and 4.0 GHz $\leq f_2 \leq$ 5.5 GHz (upper band). The surrogate models $\boldsymbol{s}_x$ and $\boldsymbol{s}_J$ are constructed using seven reference designs $\boldsymbol{x}_b^{(j)}$ corresponding to the pairs $\{f_1, f_2\}$ {2.0, 4.0}, {2.2,5.5}, {2.0, 5.5}, {2.3,4.5}, {2.4,5.5}, {2.6,4.0}, {2.7,3.5}, {2.8,4.7}, {3.0,4.0} and {3.0,3.5} (frequencies in GHz).

For verification, the procedure of Section 2 has been executed by optimizing the antenna of Figure 4 for the several target objective vectors $\boldsymbol{F}_t$ specified in Table 1. The initial design was obtained using (3). The refinement was conducted by means of the iterative scheme of Section 2.5 (cf. (7)) followed by the gradient search of (5). For benchmarking, gradient-based refinement (5) was carried out and a stand-alone procedure.

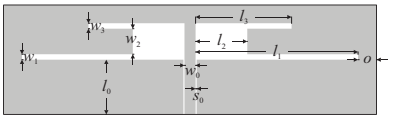

Figure 4.
Geometry of a dual-band dipole antenna (Antenna I) (Chen *et al.*, 2006)

Target operating conditions $\boldsymbol{F}_t$		Gradient-based optimization (5)		Iterative correction scheme (7)[b]	
f_1 [GHz]	f_2 [GHz]	Objective function value*	Optimization cost[a]	Objective function value*	Optimization cost[a]
2.10	4.80	–15.5 dB	9	–15.5 dB	3[$]
2.30	4.00	–17.7 dB	11	–17.5 dB	3[$]
2.45	5.10	–11.6 dB	6	–20.9 dB	3[$]
2.50	4.75	–10.6 dB	10	–21.1 dB	3[$]
2.70	4.50	–18.9 dB	11	–18.8 dB	3[$]
3.00	5.00	–22.1 dB	11	–21.3 dB	3[$]

Table 1.
Antenna I: Optimization results

Notes: *Objective function defined as the maximum reflection at both operating frequencies including their ±20 MHz vicinity. [a]The cost in terms of the number of EM simulations required by the optimization process. [b]The scheme complemented by gradient search according to (5)

Table 1 gathers the numerical results, whereas geometry parameter values of the optimized antenna can be found in Table 2. It can be observed that in all considered cases the initial designs produced by the inverse surrogate are of good quality, which demonstrates that incorporation of problem-specific knowledge (here, in the form of available pre-optimized designs) is critical to ensure the quality and reliability of the parameter adjustment process. Furthermore, it can be noted that the iterative correction yields good designs, with reflection responses well centered at the target operating frequencies for all the considered test cases. The design quality is better than that obtained using solely the gradient search. Furthermore, iterative correction is much faster: its average cost is almost three times lower than that of (5). In addition, the follow-up gradient search (also realized using (5)) does not bring much improvement as shown in Figure 5. It is only for some cases, where the additional gradient optimization slightly improves the resonance depth (especially for Case 3 and 6). This demonstrates that (7) may actually be used as the exclusive refinement technique in some cases.

3.2 Case 2: Quasi-Yagi antenna

The second verification example is a quasi-Yagi antenna (Hua *et al.*, 2015) featuring a parabolic reflector (see Figure 6) and implemented on a 1.5 mm-thick substrate. The structure is simulated in CST Microwave Studio. The geometry parameter vector is $\boldsymbol{x} = [W\ L\ L_m\ L_p\ S_d\ S_r W_2\ W_a\ W_d\ g]^T$ (all dimensions in mm). To ensure 50 ohm input impedance, the feed line width W_1 is computed for a given substrate permittivity.

For this case, the design task is formulated as follows: optimize the antenna structure for a given substrate permittivity ε_r and selected target center frequency f_0 while maintaining

Target operating conditions		Geometry parameter values [mm]					
f_1 [GHz]	f_2 [GHz]	l_1	l_2	l_3	w_1	w_2	w_3
2.10	4.80	37.2	8.220	18.7	0.29	3.62	2.39
2.30	4.00	33.5	7.12	21.3	0.60	4.68	1.11
2.45	5.10	34.0	9.64	18.9	0.34	3.06	1.75
2.50	4.75	33.1	9.20	19.8	0.45	3.57	1.28
2.70	4.50	31.1	9.71	20.8	0.36	3.89	0.71
3.00	5.00	30.1	11.1	20.4	0.50	2.85	0.85

ıle 2.
enna I: Geometry ımeter values

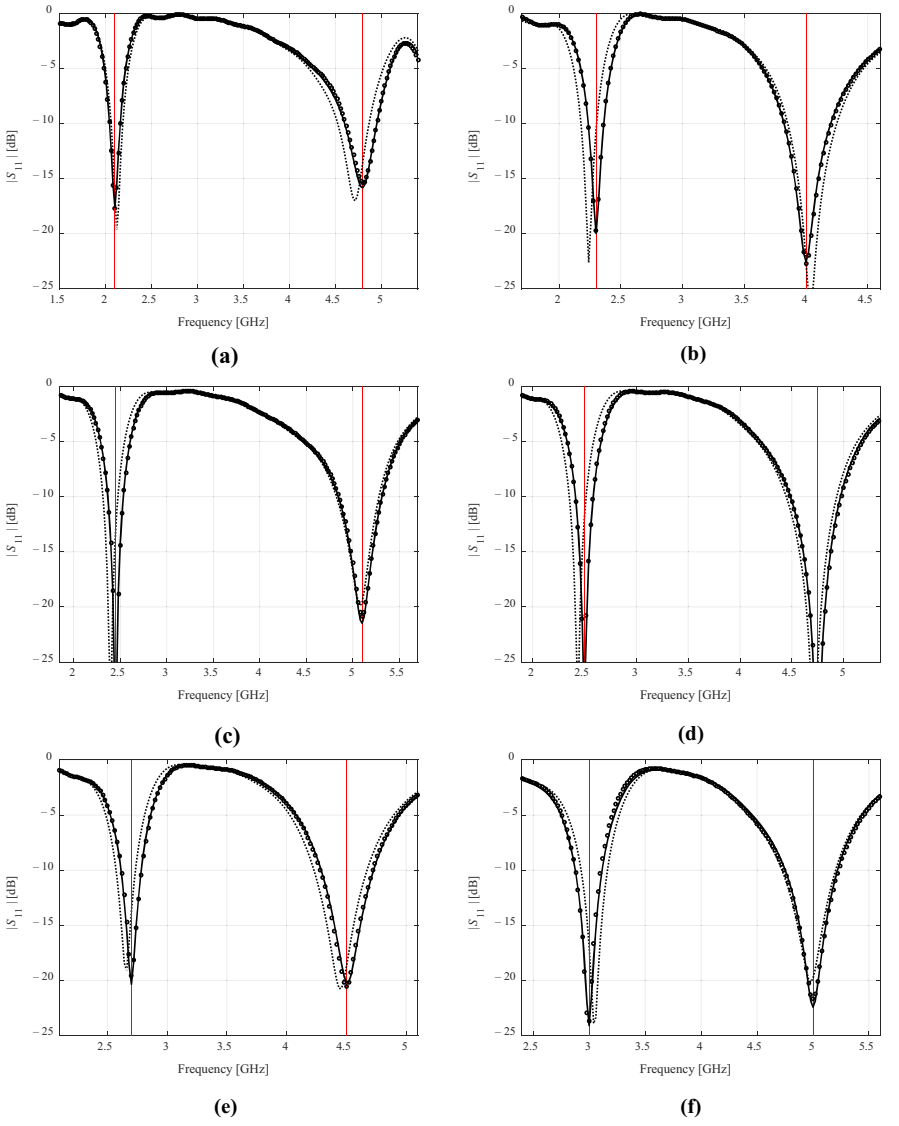

Figure 5.
Dual-band antenna responses at the initial design (. . .), the design obtained using the iterative correction scheme (o) and the final design obtained using the follow-up gradient search (5) (–)

Notes: Shown are designs corresponding to the target vectors of Table 1: (a) f1 = 2.1GHz, f2 = 4.8GHz, (b) f1 = 2.3GHz, f2 = 4.0GHz, (c) f1 = 2.45GHz, f2 = 5.1GHz, (d) f1 = 2.5GHz, f2 = 4.75 GHz, (e) f1 = 2.7 GHz, f2 = 4.5 GHz, (f) f1 = 3.0GHz, f2 = 5.0GHz.

at least 8% fractional bandwidth that is symmetric w.r.t. f_0. Additionally, the average realized gain maximization within the same 8% bandwidth is required (cf. (1)). The surrogate is to be valid for the following ranges 2.5 GHz $\leq f_1 \leq$ 5.0 GHz and 2.5 $\leq \varepsilon_{r \leq 4}$.5. Only six reference designs $\boldsymbol{x}_b^{(j)}$ are assigned: {f_1, ε_r}: {2.5,4.5}, {5.0,4.5}, {2.5,2.5}, {5.0,2.5},

{4.5,3.5} and {3.0,3.5}(frequencies in GHz). This design problem is far more challenging than the previous one due to a considerably larger number of the parameters (ten to six for the first demonstration case).

Similarly as for the first antenna, six target objective vectors $\boldsymbol{F}_t$ were selected to carry out numerical verification. The numerical results are summarized in Tables 3 and 4. Figure 7 shows the antenna responses at the initial and the optimized designs. Despite a considerably higher complexity, also, in this case, the procedure of Section 2 was able to identify the

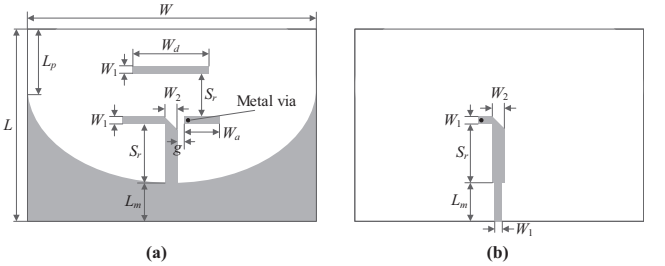

Figure 6.
Quasi-Yagi antenna with a parabolic reflector (Hua *et al.*, 2015)

Notes: (a) top layer, (b) bottom layer

Target operating conditions $\boldsymbol{F}_t$		Gradient-Based Optimization (5)		Iterative Correction Scheme (7)[b]	
f_0 [GHz]	ε_r	Average realized gain*	Optimization cost[a]	Average realized gain*	Optimization cost[a]
4.2	2.5	6.4	11	6.4	3[c]
2.45	3.2	7.0	6	7.0	3[c]
5.0	3.2	6.3	7	6.4	3[c]
3.8	3.5	5.6	11	6.1	3[c]
3.8	4.1	5.5	11	5.9	3[c]
3.0	4.4	5.5	9	5.5	3[c]

Table 3.
Antenna II: Optimization results

Notes: *Average realized gain within the fractional bandwidth of interest (here, 8%). [a]The cost in terms of the number of EM simulations required by the optimization process. [b]The scheme complemented by gradient search according to (5). [c]Cost of the iterative correction scheme (7). The average cost of the follow-up gradient search is less than four EM simulations

Target vector $\boldsymbol{F}_t$		Geometry parameter values [mm]									
f_0 [GHz]	ε_r	W	L	L_m	L_p	S_d	S_r	W_2	W_a	W_d	g
4.2	2.5	124.9	63.6	23.2	21.6	9.1	12.1	2.7	13.7	23.2	0.75
2.45	3.2	113.7	80.0	15.9	16.5	18.3	16.9	3.8	19.7	36.5	0.86
5.0	3.2	132.8	57.7	26.4	23.6	8.2	10.7	2.7	9.4	16.9	0.74
3.8	3.5	129.7	67.4	25.5	18.3	17.8	12.2	3.6	11.3	24.3	0.50
3.8	4.1	130.8	64.3	23.2	21.3	15.4	14.5	3.1	10.9	23.9	0.50
3.0	4.4	122.9	71.2	20.5	16.9	19.5	18.2	2.7	15.0	28.3	1.00

ıle 4.
enna II:
metry parameter
ıes

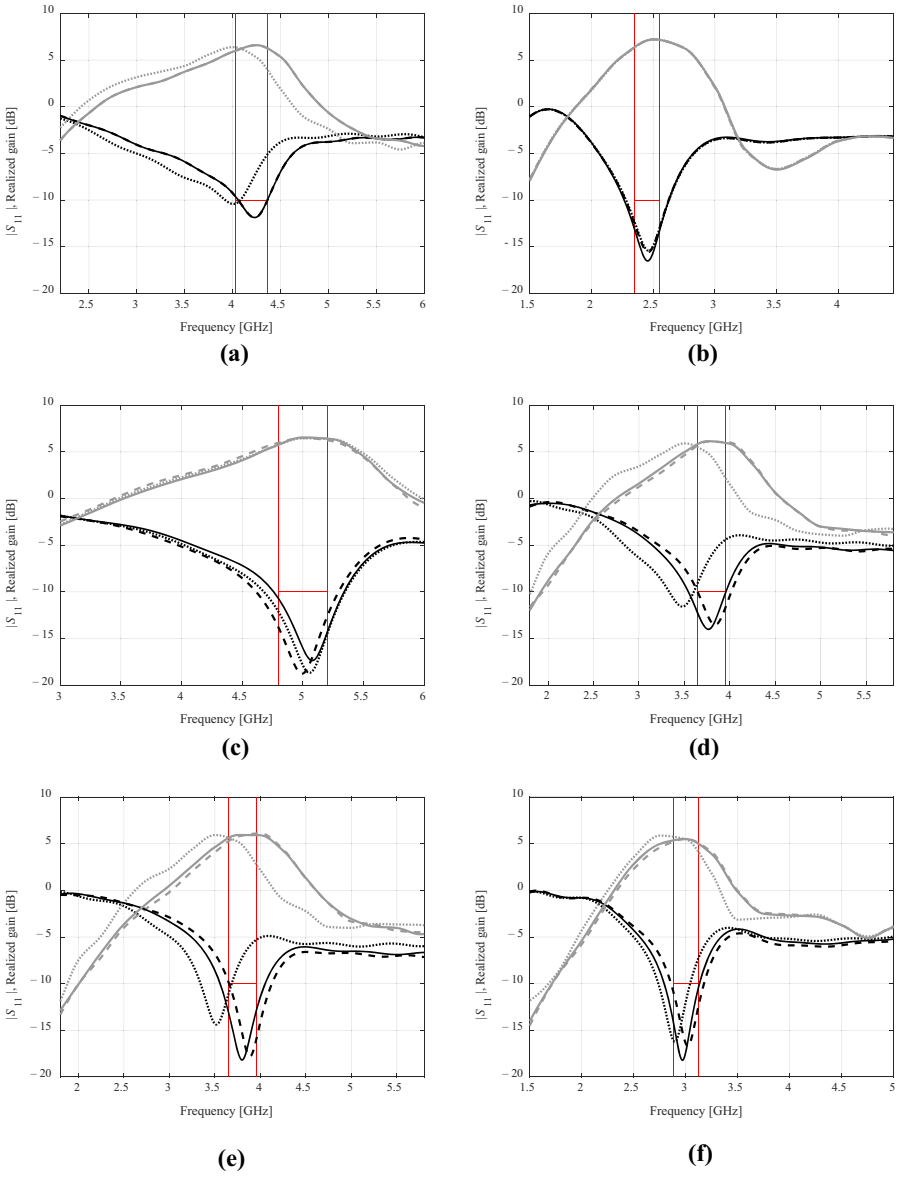

Figure 7.
Responses of Antenna II at the initial design (. . .), the designs optimized using the iterative correction scheme (. . .) and the final design obtained using the gradient search (5) (as a follow up) (–)

Notes: Shown are designs corresponding to the target vectors of Table III: (a) f1 = 3.0GHz, εr = 2.5, (b) f1 = 2.45 GHz, εr = 3.2 (c) f1 = 3.8GHz, εr = 3.5, (d) f1 = 3.8GHz, εr = 4.1, (e) f1 = 3.0GHz, εr = 4.4, (f) f1 = 4.5GHz, εr = 4.4. The antenna reflection and realized gain characteristics shown using black and gray, respectively

designs satisfying the prescribed specifications. It should be noted that the quality of the initial design produced by the surrogate model $\boldsymbol{s}_{\boldsymbol{x}}$ (cf. (3)) is not as good as for the first example. In particular, relatively considerable frequency shifts between the actual and the target operating frequencies can be observed.

Nevertheless, the proposed procedure allows for accommodating these discrepancies for all considered cases. The average cost of the iterative correction (7) is only three EM simulations, whereas the average cost of the follow-up gradient-based refinement (5) is four EM analyzes. At the same time, gradient-based only refinement is more expensive (nine EM antenna evaluations on the average) and the design quality is not as good (in Table 3, presented in terms of the average in-band gain). Also, the maximum number of iterations of (5) was set to 10 so that in most cases, the process was terminated before full convergence.

3.3 Case 3: Wideband monopole antenna

The last example is a monopole antenna (Antenna III) shown in Figure 8. The structure uses a quasi-circular radiator and modified ground plane for bandwidth enhancement (Alsath and Kanagasabai, 2015). The independent geometry parameters are $\boldsymbol{x} = [L_0\ dR\ Rr_{rel}\ dL\ d_w\ L_g\ L_1\ R_1 dr\ c_{rel}]^T$. The feed line width is computed for given substrate parameters

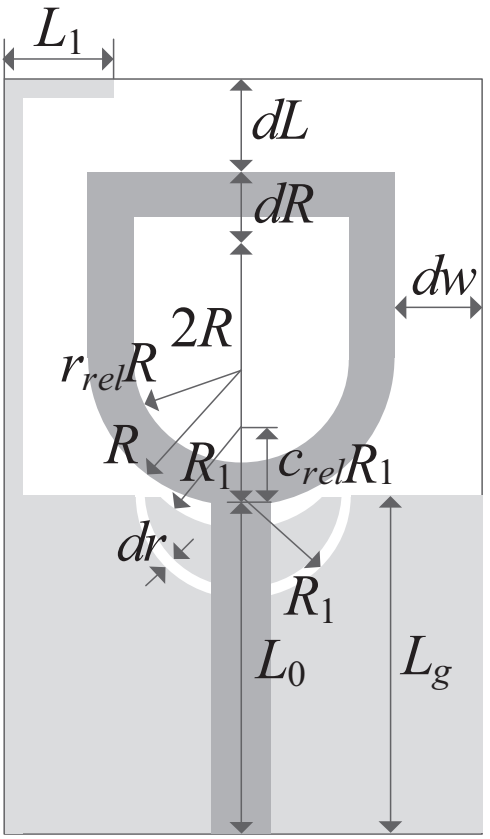

ure 8.
metry of the
B monopole
nna (Alsath and
agasabai, 2015);
t gray shades
w ground plane

(permittivity and height) to ensure 50 Ohm impedance. The computational model is implemented in CST Microwave Studio and evaluated using its transient solver (~380.000 mesh cells, simulation time 1 min). The model incorporates the SMA connector. The antenna is supposed to operate within the UWB frequency range from 3.1 GHz to 10.6 GHz. Design optimality is understood as the minimization of the maximum in-band reflection.

The objective is to re-design the antenna for any dielectric substrate within the following ranges: permittivity $2.0 \leq \varepsilon_r \leq 5.0$ and height $0.5\,\text{mm} \leq h \leq 1.5\,\text{mm}$. There are five reference designs pre-optimized for the following pairs $\{\varepsilon_r, h\} = \{3.5,1.0\}, \{2.0,0.5\}, \{2.0,1.5\}, \{5.0,0.5\}$ and $\{5.0,1.5\}$.

Tables 5 and 6 gather the numerical results obtained for six target substrate parameter vectors, whereas Figure 9 shows the antenna responses. In this case, the initial designs of (3) are of high quality so that gradient-based refinement (5) is sufficient. As a matter of fact, the application of the iterative scheme (7) is not possible here because the substrate parameters can be considered as operating conditions rather than figures of interest. This example was included specifically to indicate potential limitations of the scope of the presented method. Notwithstanding, indirect application of (7) is possible by translating potential frequency shifts into the appropriate (overall) scaling of the antenna parameters; however, there is no need to do that for Antenna III due to the aforementioned high quality of the initial designs.

4. Experimental validation

Selected optimized designs, one for each of Antennas I through III, have been fabricated for additional validation. For Antenna I, this is a design corresponding to the target operating

Target operating conditions $\boldsymbol{F}_t$			
ε_r	h [mm]	Objective function value*	Optimization cost[a]
2.2	0.76	–12.8 dB	6
3.0	0.76	–13.3 dB	9
4.4	1.5	–15.6 dB	7
2.5	1.5	–19.7 dB	8
3.38	0.76	–13.7 dB	9
3.38	1.5	–18.1 dB	8

Notes: *Maximum reflection within the frequency range from 3.1 GHz to 10.6 GHz. [a]The cost in terms of the number of EM simulations required by the optimization process

Table 5.
Antenna III: Optimization results

Target vector $\boldsymbol{F}_t$		Geometry parameter values [mm]										
ε_r	h [mm]	L	dR	R	r_{rel}	dL	dw	L_g	L_1	R_1	dr	c_{rel}
2.2	0.76	12.2	0.06	6.91	0.21	3.26	5.37	12.4	3.45	3.06	0.29	0.71
3.0	0.76	11.8	0.11	6.43	0.28	3.85	5.97	11.7	2.01	2.34	0.42	0.20
4.4	1.5	12.8	0.00	5.48	0.10	4.54	6.96	12.3	1.56	2.51	0.29	0.90
2.5	1.5	12.2	0.02	6.76	0.13	5.00	5.69	12.4	1.96	3.84	0.20	0.52
3.38	0.76	11.8	0.12	6.09	0.16	3.95	6.14	11.6	2.29	2.16	0.43	0.39
3.38	1.5	12.1	0.01	5.71	0.29	4.86	6.03	11.9	2.08	3.65	0.24	0.87

Note: *Variables with subscript *rel* are relative, i.e. unitless

Table 6.
Antenna III: Geometry parameter values

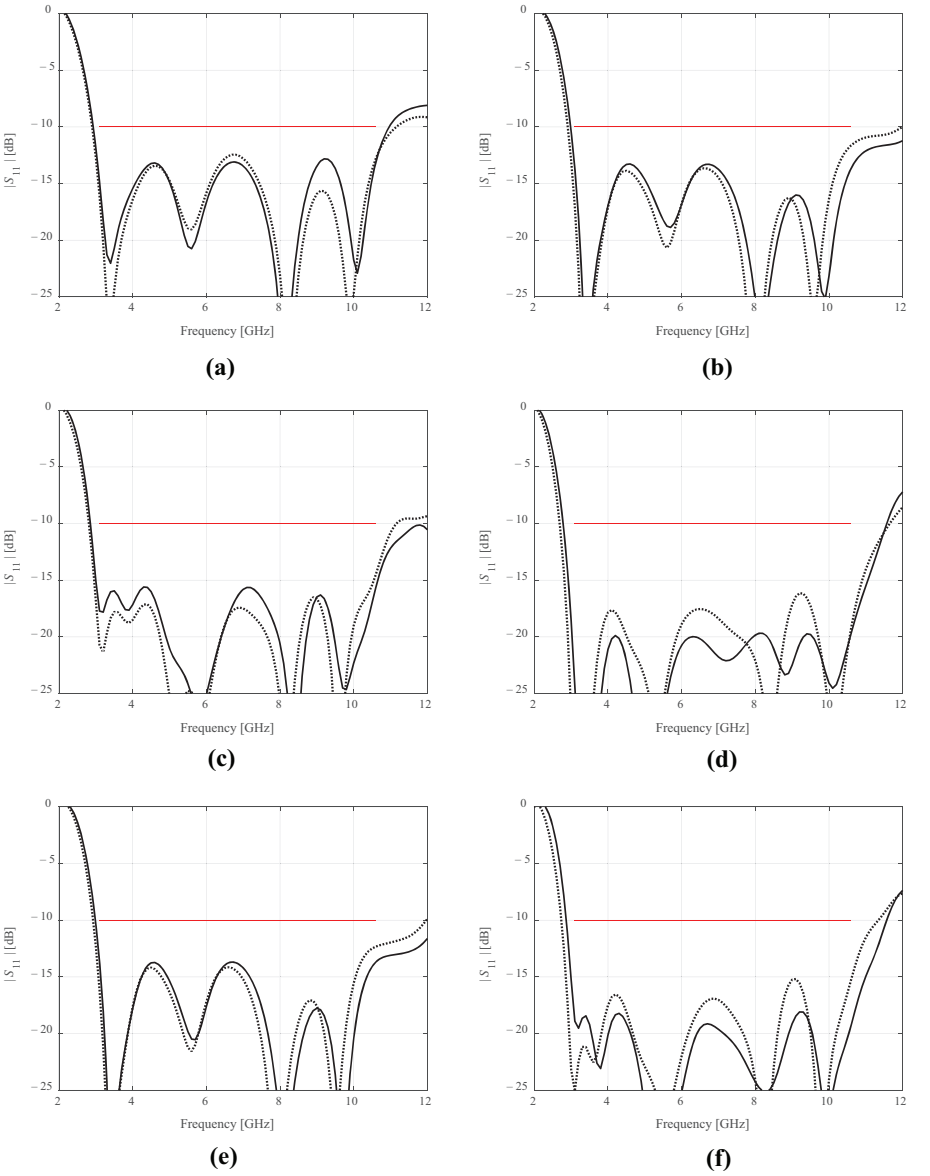

Figure 9.
ponses of
enna III at the
al design (. . .) and
final design
ined using the
lient search (5)

Notes: Shown are designs corresponding to the target vectors of Table 5: (a) ε = 2.2, h = 0.76 mm, (b) ε = 3.0, h = 0.76 mm, (c) ε = 4.4, h = 1.5 mm, (d) ε = 2.5, h = 1.5 mm, (e) ε = 3.38, h = 0.76 mm, (f) ε = 3.38, h = 1.5mm. The design specifications marked using the horizontal line

frequencies f_1 = 2.45 GHz and f_2 = 5.1 GHz, implemented on 0.76 mm-thick RO4350 substrate. In the case of Antenna II, the design optimized for f_0 = 4.2 GHz and ε_r = 2.5 has been fabricated on a 1.5 mm thick AD250 substrate. For Antenna III, the design optimized for ε_r = 4.4 and h = 1.5 mm has been selected and implemented on FR4 laminate.

Figures 10–12 show the photographs of the antenna prototypes, as well as the comparison of simulated and measured characteristics. The agreement between both data sets is generally good for all considered structures. Small discrepancies can be attributed to the measurement setup (e.g. 90-degree bends used to mount the antennas for E-plane pattern evaluation) or the lack of SMA connectors in computational models (except for Antenna III).

5. Conclusions

The paper presented a knowledge-based framework for accelerated design optimization of antenna structures. One of the fundamental components of our procedure is machine learning tools in the form of the inverse and forward kriging metamodels, which are set up using the available designs of the antenna at hand and used to yield an initial design for further refinement. While the second component is an iterative correction scheme, which permits rapid accommodation of the initial design discrepancies (with respect to the target performance figure values), primarily the frequency shifts. The gradient-based optimizer is also incorporated to accomplish fine-tuning of the parameter in the final stage of the procedure.

Our methodology has been comprehensively validated using three-antenna examples of various characteristics: narrow-band, dual-band and wideband, which, in turn, have been

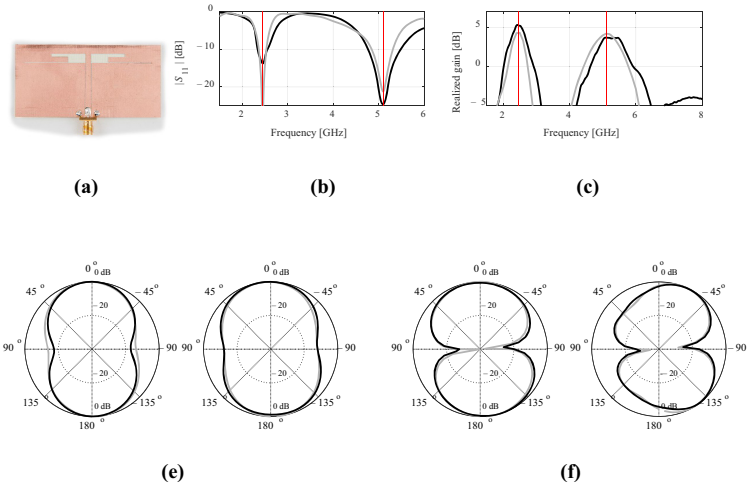

Notes: (a) Photographs of the prototype, (b) reflection responses, (c) realized gain characteristics, (d) H-plane radiation patterns (from left to right: f1 = 2.45 GHz, f1 = 5.1GHz, (e) E-plane radiation patterns (f1 = 2.45 GHz and f = 5.1GHz on the left- and right-hand-side, respectively). Simulations and measurements shown as gray and black curves, respectively. Red lines in (b) and (c) indicate the target operating frequencies.

Figure 10. Antenna I optimized for f_1 = 2.45 GHz and f_2 = 5.1 GHz, implemented on RO4350 substrate

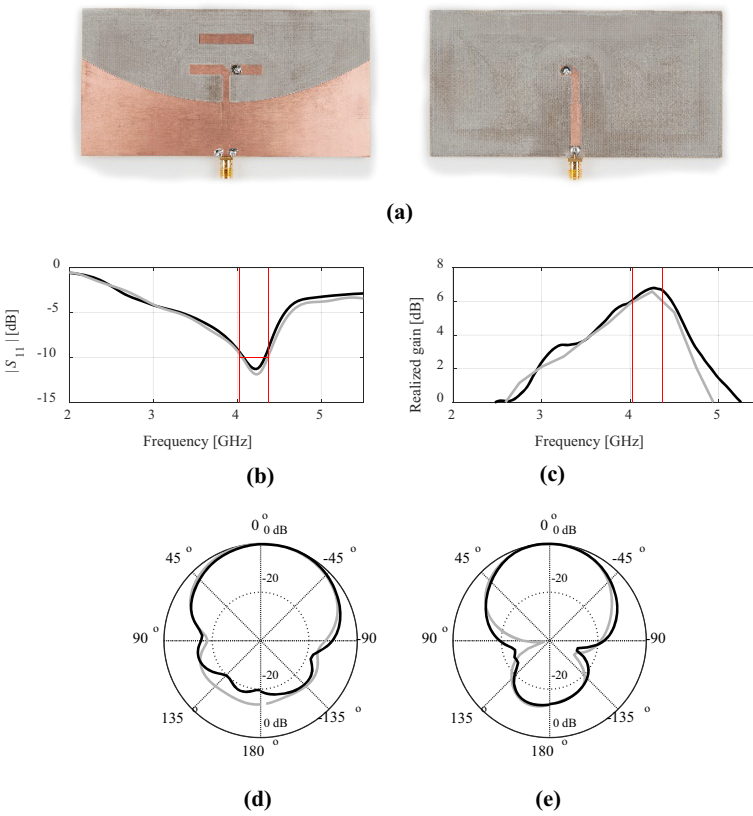

Figure 11.
Antenna II optimized for $f_0 = 4.2$ GHz and $\varepsilon_{r=2}.5$; the structure implemented on AD250 substrate

Notes: (a) photographs of the prototype, (b) reflection responses, (c) realized gain characteristics, (d) xy-plane radiation pattern at 4.2 Ghz (y is the end-fire direction), (e) zy-plane radiation pattern at 4.2 Ghz. Simulations and measurements shown as gray and black curves, respectively. Red lines in (b) and (c) denote the intended operating band.

optimized under different scenarios. The numerical results obtained for a number of target objective vectors are consistent throughout the considered test set. The presented framework is demonstrably capable of yielding optimized antenna designs at the cost of just a handful of EM simulations. The practical importance of the iterative correction procedure has been corroborated through a comparison with gradient-only refinement. It has been found that the incorporation of the problem-specific knowledge into the optimization framework, encoded using machine learning techniques, is a critical component that both facilitates the parameter adjustment process and renders it considerably more reliable.

The proposed approach can be a viable tool to expedite the antenna design closure if either a certain number of previously obtained designs are available or the designer finds the initial effort of preparing the design database justifiable (e.g. by the intended multiple re-uses of the procedure).

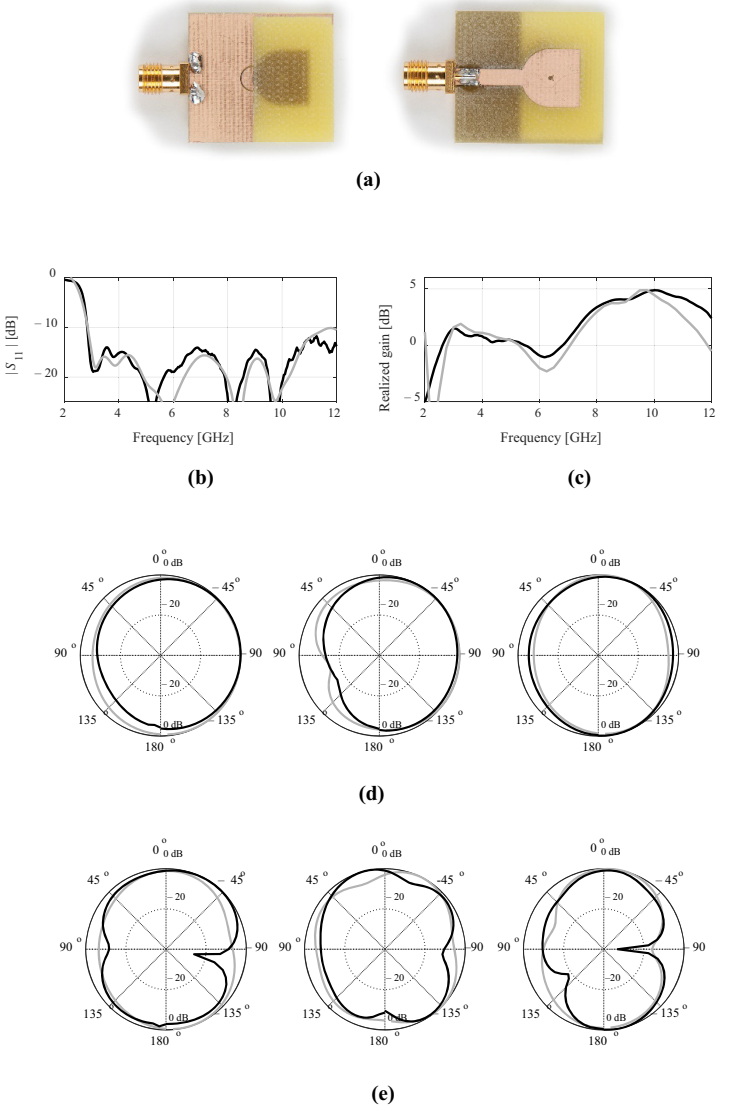

Notes: (a) photograph of the antenna prototype, (b) reflection responses, (c) realized gain characteristics, (d) H-plane radiation patterns (from left to right: 4 GHz, 6 GHz, 8 GHz), (e) E-plane radiation patterns (from left to right: 4 GHz, 6 GHz, 8 GHz). Simulations and measurements shown as gray and black curves, respectively.

Figure 12.
Antenna III optimized for $\varepsilon_{r=4}$.4 and $h = 1.5$ mm, implemented on FR4 substrate

References

Aldhafeeri, A. and Rahmat-Samii, Y. (2019), "Brain storm optimization for electromagnetic applications: continuous and discrete", *IEEE Transactions on Antennas and Propagation*, Vol. 67 No. 4, pp. 2710-2722, doi: 10.1109/TAP.2019.2894318.

Alsath, M.G.N. and Kanagasabai, M. (2015), "Compact UWB monopole antenna for automotive communications", *IEEE Transactions on Antennas and Propagation*, Vol. 63 No. 9, pp. 4204-4208, doi: 10.1109/TAP.2015.2447006.

Alzahed, A.M., Mikki, S.M. and Antar, Y.M.M. (2019), "Nonlinear mutual coupling compensation operator design using a novel electromagnetic machine learning paradigm", *IEEE Antennas and Wireless Propagation Letters*, Vol. 18 No. 5, pp. 861-865, doi: 10.1109/LAWP.2019.2903787.

Arndt, B.F. (2012), "WASP-NET: recent advances in fast EM CAD and optimization of waveguide components, feeds, and aperture antennas", *IEEE International Symposium on Antennas and Propagation, 8-14 July, 2012, Chicago, IL*, doi: 10.1109/APS.2012.6348420

Baratta, I.A., de Andrade, C.B., de Assis, R.R. and Silva, E.J. (2018), "Infinitesimal dipole model using space mapping optimization for antenna placement", *IEEE Antennas and Wireless Propagation Letters*, Vol. 17 No. 1, pp. 17-20, doi: 10.1109/LAWP.2017.2771721.

Bhattacharya, R., Garg, R. and Bhattacharyya, T.K. (2016), "Design of a PIFA-driven compact yagi-type pattern diversity antenna for handheld devices", *IEEE Antennas and Wireless Propagation Letters*, Vol. 15, pp. 255-258, doi: 10.1109/LAWP.2015.2440260.

Broyden, C.G. (1965), "A class of methods for solving nonlinear simultaneous equations", *Mathematics of Computation*, Vol. 19 No. 92, pp. 577-593.

Caenepeel, M., Ferranti, F. and Rolain, Y. (2016), "Efficient and automated generation of multidimensional design curves for coupler-resonator filters using system identification and metamodels", *International Conference on Synthesis, Modeling, Analysis and Simulation Methods and Applications to Circuit Design (SMACD), 27-30 June, 2016, Lisbon*, doi: 10.1109/SMACD.2016.7520717

Chen, Y.C., Chen, S.Y. and Hsu, P. (2006), "Dual-band slot dipole antenna fed by a coplanar waveguide", *IEEE International Symposium on Antennas and Propagation, 9-14 July, 2006*, pp. 3589-3592, *Albuquerque, NM*, doi: 10.1109/APS.2006.1711396

Choi, K., Jang, D.H., Kang, S.I., Lee, J.H., Chung, T.K. and Kim, H.S. (2016), "Hybrid algorithm combining genetic algorithm with evolution strategy for antenna design", *IEEE Transactions on Magnetics*, Vol. 52 No. 3, pp. 1-4, doi: 10.1109/TMAG.2015.2486043.

Conn, N.I.M., Gould, A.R. and Toint, P.L. (2000), *Trust Region Methods*, MPS-SIAM Series on Optimization, Philadelphia, PA.

Connell, I.R.O. and Menon, R.S. (2019), "Shape optimization of an electric dipole array for 7 tesla neuroimaging", *IEEE Transactions on Medical Imaging*, Vol. 38 No. 9, pp. 2177-2187, doi: 10.1109/TMI.2019.2906507.

Deshmukh, A.A., Verma, P. and Pawar, S. (2019), "Variations of P-shape microstrip antennas for multi-band dual polarised response", *IET Microwaves, Antennas and Propagation*, Vol. 13 No. 3, pp. 398-405, doi: 10.1049/iet-map.2018.5333.

Dong, J., Qin, W. and Wang, M. (2019), "Fast multi-objective optimization of multi-parameter antenna structures based on improved BPNN surrogate model", *IEEE Access*, Vol. 7, pp. 77692-77701, doi: 10.23919/ACESS.2018.8669367.

Du, J. and Roblin, C. (2018), "Stochastic surrogate models of deformable antennas based on vector spherical harmonics and polynomial chaos expensions: application to textile antennas", *IEEE Transactions on Antennas and Propagation*, Vol. 66 No. 7, pp. 3610-3622, doi: 10.1109/TAP.2018.2829820.

Easum, J.A., Nagar, J., Werner, P.L. and Werner, D.H. (2018), "Efficient multi-objective antenna optimization with tolerance analysis through the use of surrogate models", *IEEE Transactions on Antennas and Propagation*, Vol. 66 No. 12, pp. 6706-6715, doi: 10.1109/TAP.2018.2870338.

Fakih, M.A., Diallo, A., Le Thuc, P., Staraj, R., Mourad, O. and Rachid, E.A. (2019), "Optimization of efficient dual band PIFA system for MIMO half-duplex 4G/LTE and full-duplex 5G communications", *IEEE Access*, Vol. 7, pp. 128881-128895, doi: 10.1109/ACCESS.2019.2940556.

Felicio, J.M., Bioucas-Dias, J.M., Costa, J.R. and Fernandes, C.A. (2019), "Antenna design and near-field characterization for medical microwave imaging applications", *IEEE Transactions on Antennas and Propagation*, Vol. 67 No. 7, pp. 4811-4824, doi: 10.1109/TAP.2019.2905742.

Goudos, S.K., Siakavara, K., Samaras, T., Vafiadis, E.E. and Sahalos, J.N. (2011), "Self-adaptive differential evolution applied to real-valued antenna and microwave design problems", *IEEE Transactions on Antennas and Propagation*, Vol. 59 No. 4, pp. 1286-1298, doi: 10.1109/TAP.2011.2109678.

Han, Z.J., Song, W. and Sheng, X.Q. (2017), "Gain enhancement and RCS reduction for patch antenna by using polarization-dependent EBG surface", *IEEE Antennas and Wireless Propagation Letters*, Vol. 16, pp. 1631-1634, doi: 10.1109/LAWP.2017.2658195.

Hassan, E., Noreland, D., Augustine, R., Wadbro, E. and Berggren, M. (2015), "Topology optimization of planar antennas for wideband near-field coupling", *IEEE Transactions on Antennas and Propagation*, Vol. 63 No. 9, pp. 4208-4213, doi: 10.1109/TAP.2015.2449894.

Hua, Z., Haichuan, G., Hongmei, L., Beijia, L., Guanjun, L. and Qun, W. (2015), "A novel high-gain quasi-Yagi antenna with a parabolic reflector", *IEEE International Symposium on Antennas and Propagation (ISAP), 9-12 Nov., 2015, Hobart*.

Huang, H.J., Tsai, C.H., Lai, C.P. and Chen, S.Y. (2015), "Frequency-tunable miniaturized strip loop antenna fed by a coplanar strip", *IEEE Antennas and Wireless Propagation Letters*, Vol. 15, pp. 1000-1003, doi: 10.1109/LAWP.2015.2490059.

Jacobs, J.P. (2012), "Bayesian support vector regression with automatic relevance determination kernel for modeling of antenna input characteristics", *IEEE Transactions on Antennas and Propagation*, Vol. 60 No. 4, pp. 2114-2118, doi: 10.1109/LAWP.2015.2490059.

Jacobs, J.P. and Koziel, S. (2014), "Two-stage framework for efficient Gaussian process modeling of antenna input characteristics", *IEEE Transactions on Antennas and Propagation*, Vol. 62 No. 2, pp. 706-713, doi: 10.1109/TAP.2013.2290121.

Kim, S. and Nam, S. (2019), "A compact and wideband linear array antenna with low mutual coupling", *IEEE Transactions on Antennas and Propagation*, Vol. 67 No. 8, pp. 5695-5699, doi: 10.1109/TAP.2019.2922833.

Kouassi, A., Nguyen-Trong, N., Kaufmann, T., Lallechere, S., Bonnet, P. and Fumeaux, C. (2016), "Reliability-aware optimization of a wideband antenna", *IEEE Transactions on Antennas and Propagation*, Vol. 64 No. 2, pp. 450-460, doi: 10.1109/TAP.2015.2508482.

Koziel, S. (2015), "Fast simulation-driven antenna design using response-feature surrogates", *International Journal of RF and Microwave Computer-Aided Engineering*, Vol. 25 No. 5, pp. 394-402, doi: 10.1002/mmce.20873.

Koziel, S. and Pietrenko-Dabrowska, A. (2019a), "Variable-fidelity simulation models and sparse gradient updates for cost-efficient optimization of compact antenna input characteristics", *Sensors*, Vol. 19 No. 8, doi: 10.3390/s19081806.

Koziel, S. and Pietrenko-Dabrowska, A. (2019b), "Reduced-cost electromagnetic-driven optimization of antenna structures by means of trust-region gradient-search with sparse Jacobian updates", *IET Microwaves, Antennas and Propagation*, Vol. 13 No. 10, pp. 1646-1652, doi: 10.1049/iet-map.2018.5879.

Koziel, S. and Unnsteinsson, S.D. (2018), "Expedited design closure of antennas by means of trust-region-based adaptive response scaling", *IEEE Antennas and Wireless Propagation Letters*, Vol. 17 No. 6, pp. 1099-1103, doi: 10.1109/LAWP.2018.2834145.

Kumar, P., Dwari, S., Saini, R.K. and Mandal, M.K. (2019), "Dual-band dual-sense polarization reconfigurable circularly polarized antenna", *IEEE Antennas and Wireless Propagation Letters*, Vol. 18 No. 1, pp. 64-68, doi: 10.1109/LAWP.2018.2880799.

Lalbakhsh, A., Afzal, M.U. and Esselle, K.P. (2017), "Multiobjective particle swarm optimization to design a time-delay equalizer metasurface for an electromagnetic band-gap resonator antenna", *IEEE Antennas and Wireless Propagation Letters*, Vol. 16, pp. 915-915, doi: 10.1109/LAWP.2016.2614498.

Leifsson, L. and Koziel, S. (2014), "Inverse airfoil design using variable-resolution models and shape-preserving response prediction", *Aerospace Science and Technology*, Vol. 39, pp. 513-522, doi: 10.1016/j.ast.2014.05.013.

Li, W., Wang, Y., You, B., Shi, Z. and Liu, Q.H. (2018), "Compact ring slot antenna with harmonic suppression", *IEEE Antennas and Wireless Propagation Letters*, Vol. 17 No. 12, pp. 2459-2463, doi: 10.1109/LAWP.2018.2877974.

Liao, W.J., Hsieh, C.Y., Dai, B.Y. and Hsiao, B.R. (2015), "Inverted-F/slot integrated dual-band four-antenna system for WLAN access point", *IEEE Antennas and Wireless Propagation Letters*, Vol. 14, pp. 847-850, doi: 10.1109/LAWP.2014.2381362.

Mendes, C. and Peixeiro, C. (2018), "On-body transmission performance of a novel dual-model wearable microstrip antenna", *IEEE Transactions on Antennas and Propagation*, Vol. 66 No. 9, pp. 4872-4877, doi: 10.1109/TAP.2018.2851669.

Mishra, S., Yadav, R.N. and Singh, R.P. (2015), "Directivity estimations for short dipole antenna arrays using radial basis function neural networks", *IEEE Antennas and Wireless Propagation Letters*, Vol. 14, pp. 1219-1222, doi: 10.1109/LAWP.2015.2399453.

Queipo, N.V., Haftka, R.T., Shyy, W., Goel, T., Vaidynathan, R. and Tucker, P.K. (2005), "Surrogate-based analysis and optimization", *Progress in Aerospace Sciences*, Vol. 41 No. 1, pp. 1-28, doi: 10.1016/j.paerosci.2005.02.001.

Salam, A., Vuran, M.C., Dong, X., Argyropoulos, C. and Irmak, S. (2019), "A theoretical model of underground dipole antennas for communications in internet of underground things", *IEEE Transactions on Antennas and Propagation*, Vol. 67 No. 6, pp. 3996-4009, doi: 10.1109/TAP.2019.2902646.

Saurav, K., Mallat, N.K. and Antar, Y.M.M. (2018), "A three-port polarization and pattern diversity ring antenna", *IEEE Antennas and Wireless Propagation Letters*, Vol. 17 No. 7, pp. 1324-1328, doi: 10.1109/LAWP.2018.2844170.

Tak, J., Kantemur, A., Sharma, Y. and Xin, H. (2018), "A 3-D-printed W-band slotted waveguide array antenna optimized using machine learning", *IEEE Antennas and Wireless Propagation Letters*, Vol. 17 No. 11, pp. 2008-2012, doi: 10.1109/LAWP.2018.2857807.

Torun, H.M. and Swaminathan, M. (2019), "High-dimensional global optimization method for high-frequency electronic design", *IEEE Transactions on Microwave Theory and Techniques*, Vol. 67 No. 6, pp. 2128-2142, doi: 10.1109/TMTT.2019.2915298.

Tsukamoto, K. and Arai, H. (2016), "Optimization of smooth walled horn antenna using multilevel fast multipole method", *IEEE International Symposium on Antennas and Propagation (ISAP), 24-28 Oct. 2016, Okinawa*.

Ullah, U. and Koziel, S. (2018), "A broadband circularly polarized wide-slot antenna with a miniaturized footprint", *IEEE Antennas and Wireless Propagation Letters*, Vol. 17 No. 12, pp. 2454-2458, doi: 10.1109/LAWP.2018.2877800.

Ullah, U., Koziel, S. and Mabrouk, I.B. (2020), "Rapid redesign and bandwidth/size tradeoffs for compact wideband circular polarization antennas using inverse surrogates and fast EM-based parameter tuning", *IEEE Transactions on Antennas and Propagation*, Vol. 68 No. 1, pp. 81-89, doi: 10.1109/TAP.2019.2935817.

Wang, J., Yang, X.S. and Wang, B.Z. (2018), "Efficient gradient-based optimization of pixel antenna with large-scale connections", *IET Microwaves, Antennas and Propagation*, Vol. 12 No. 3, pp. 385-389, doi: 10.1049/iet-map.2017.0719.

Wu, J. and Sarabandi, K. (2017), "Compact omnidirectional circularly polarized antenna", *IEEE Transactions on Antennas and Propagation*, Vol. 65 No. 4, pp. 1550-1557, doi: 10.1109/TAP.2017.2669959.

Xu, Y., Wang, J., Ge, L., Wang, X. and Wu, W. (2018), "Design of a notched-band vivaldi antenna with high selectivity", *IEEE Antennas and Wireless Propagation Letters*, Vol. 17 No. 1, pp. 62-65, doi: 10.1109/LAWP.2017.2773707.

Zeng, J. and Luk, K.M. (2019), "Single-layered broadband magnetoelectric dipole antenna for new 5G application", *IEEE Antennas and Wireless Propagation Letters*, Vol. 18 No. 5, pp. 911-915, doi: 10.1109/LAWP.2019.2905768.

About the authors

Slawomir Koziel received the MSc and PhD degrees in electronic engineering from Gdansk University of Technology, Poland, in 1995 and 2000, respectively. He also received the MSc degrees in theoretical physics and in mathematics, in 2000 and 2002, respectively, as well as the PhD in mathematics in 2003, from the University of Gdansk, Poland. He is currently a Professor at the School of Science and Engineering, Reykjavik University, Iceland. His research interests include CAD and modeling of microwave and antenna structures, simulation-driven design, surrogate-based optimization, space mapping, circuit theory, analog signal processing, evolutionary computation and numerical analysis.

Anna Pietrenko-Dabrowska received the MSc and PhD degrees in electronic engineering from Gdansk University of Technology, Poland, in 1998 and 2007, respectively. Currently, she is an Associate Professor with Gdansk University of Technology, Poland. Her research interests include simulation-driven design, design optimization, control theory, modeling of microwave and antenna structures, numerical analysis. Anna Pietrenko-Dabrowska is the corresponding author and can be contacted at: anndabr1@pg.edu.pl